Journal of Integrative Agriculture 2022, 21(10): 2805–2817

Available online at www.sciencedirect.com

ScienceDirect

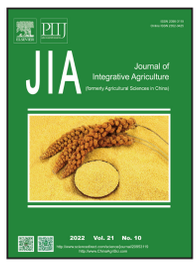

RESEARCH ARTICLE

Genetic dissection of the grain-filling rate and related traits through linkage analysis and genome-wide association study in bread wheat

YU Hai-xia[1*], DUAN Xi-xian[1*], SUN Ai-qing[1], SUN Xiao-xiao[1], ZHANG Jing-juan[2], SUN Hua-qing[3], SUN Yan-yan[1], NING Tang-yuan[1], TIAN Ji-chun[1], WANG Dong-xue[1], LI Hao[1], FAN Ke-xin[1], WANG Ai-ping[2], MA Wu-jun[4], CHEN Jian-sheng[1]

[1] *State Key Laboratory of Crop Biology/Key Laboratory of Crop Water Physiology and Drought-tolerance Germplasm Improvement, Minstry of Agriculture and Rural Affairs/Group of Wheat Quality Breeding, College of Agronomy, Shandong Agricultural University, Tai'an 271018, P.R.China*

[2] *Dezhou Agricultural Protection and Technological Extension Center, Dezhou 253000, P.R.China*

[3] *Zhongnong Tiantai Seed Co., Ltd., Pingyi 273300, P.R.China*

[4] *School of Veterinary and Life Sciences, Murdoch University, Murdoch, WA 6150, Australia*

Abstract

Wheat grain yield is generally sink-limited during grain filling. The grain-filling rate (GFR) plays a vital role but is poorly studied due to the difficulty of phenotype surveys. This study explored the grain-filling traits in a recombinant inbred population and wheat collection using two highly saturated genetic maps for linkage analysis and genome-wide association study (GWAS). Seventeen stable additive quantitative trait loci (QTLs) were identified on chromosomes 1B, 4B, and 5A. The linkage interval between *IWB19555* and *IWB56078* showed pleiotropic effects on GFR_1, GFR_{max}, kernel length (KL), kernel width (KW), kernel thickness (KT), and thousand kernel weight (TKW), with the phenotypic variation explained (PVE) ranging from 13.38% (KW) to 33.69% (TKW). 198 significant marker-trait associations (MTAs) were distributed across most chromosomes except for 3D and 4D. The major associated sites for GFR included *IWB44469* (11.27%), *IWB8156* (12.56%) and *IWB24812* (14.46%). Linkage analysis suggested that *IWB35850*, identified through GWAS, was located in approximately the same region as *QGFRmax2B.3-11*, where two high-confidence candidate genes were present. Two important grain weight (GW)-related QTLs colocalized with grain-filling QTLs. The findings contribute to understanding the genetic architecture of the GFR and provide a basic approach to predict candidate genes for grain yield trait QTLs.

Keywords: wheat, grain-filling rate, linkage analysis, genome-wide association study

Received 25 February, 2021 Accepted 6 July, 2021

YU Hai-xia, E-mail: yuhaixia66@163.com; DUAN Xi-xian, E-mail: 1278901428@qq.com; Correspondence CHEN Jian-sheng, Tel: +86-538-8241959, E-mail: jshch@sdau.edu.cn; MA Wu-jun, E-mail: W.Ma@murdoch.edu.au

[*] These authors contributed equally to this study.

doi: 10.1016/j.jia.2022.07.032

1. Introduction

Wheat is one of the most important grain crops in the world. A high grain yield is the predominant objective of breeding programs aimed at meeting the growing demand for wheat imposed by the ever-growing human

population. The spike number per unit area, kernel number per spike (KN), and thousand kernel weight (TKW) are the three basic yield components (Li and Gill 1970; Gupta *et al.* 2006; Fischer 2008, 2011; Dobrovolskaya *et al.* 2015). These components can be further divided into more integrant elements, which are determined by many factors. Among these elements, the grain-filling duration (GFD) and rate (GFR) are the main determinants influencing individual kernel size and TKW, and ultimately affecting the final grain yield (Wang R X *et al*. 2008; Alonso *et al.* 2018; Baillot *et al*. 2018).

The GFD is highly variable depending on meteorological factors, such as temperature, relative humidity, and the presence of stress (Wiegand and Cuellar 1981; Knott and Gebeyehou 1987; Dfreynolds *et al.* 2000; Wang *et al.* 2009). GFR is relatively stable and is less affected by environmental factors (Sanford *et al.* 1985; Mashiringwani *et al.* 1994), indicating that a high GFR is achievable through genetic breeding. Under adverse conditions such as abiotic and biotic stresses, varieties with high-filling rates perform better in general, producing fuller seeds and showing lower effects of stress than varieties with low-filling rates. The dry weight of wheat grain increases in a pattern corresponding to an S-shaped curve during grain filling, and the entire period can be divided into the following three stages: an increasing period, a rapidly increasing period, and a slowly increasing period. Within a given environment, grain-filling characteristics are largely determined by genetic factors (Zhu *et al.* 2019). Therefore, identifying genetic loci or genes that control the GFR can contribute to the effective breeding of high-yield wheat cultivars.

Several genes related to grain weight (GW) have been isolated in rice. Among these genes, *GIF1* (*Grain Incomplete Filling 1*) encodes a cell-wall invertase required for carbon partitioning during early grain filling (Yano 2001; Wang E T *et al.* 2008). Wang *et al.* (2012) identified the QTL *GW8*, which is synonymous with the *OsSPL16* gene, encoding a positive regulator of cell proliferation. Higher expression of *OsSPL16* promotes cell division and grain filling, leading to a greater grain width and yield in rice. Li *et al.* (2016) used the CRISPR/Cas9 system to mutate the *GS3* (*Os03g0407400*) gene in the rice cultivar Zhonghua 11, which further confirmed its function as a regulator of grain size. Zhang Y *et al.* (2018) found that *TaGW2-B1* and *TaGW2-D1* could regulate wheat grain size by adjusting the number and length of exocarp cells in developing seeds. *TaGASR7-A1* was homologously cloned and affects grain weight by controlling grain length (Zhang *et al.* 2015). Tollenaar and Lee (2006) examined the physiological processes associated with genetic gain and heterosis in maize. Their results revealed that the genetic gain was not associated with changes in the harvest index because the increase in the kernel number and the increase in dry matter accumulation during the grain-filling period were proportional, whereas in heterosis, the increase in the kernel number was much greater than the increase in dry matter accumulation during the grain-filling period.

Despite the importance and high breeding value, only a few reports have focused on the identification of genetic factors or QTL mapping for the wheat GFR. QTLs of GFR and related traits were observed on chromosomes 2A, 3B, 4A, 5A, 5DL, and 7B (Xie *et al.* 2015), which is largely due to the highly time-consuming nature of accurate phenotype surveys. The large, complex polyploid genome has also been a factor restricting good grain filling research in wheat in the past (Consortium 2014). However, due to the low density of the genetic linkage map, which was limited by the technology available at the time, the reported QTL regions were rather large, without closely linked markers. There are still few available reports addressing genes for GFR in wheat.

In recent decades, most complex quantitative traits have been evaluated based on genetic linkage maps (Zhang Z H *et al.* 2013; Du *et al*. 2019). This strategy presents the advantage of more efficient macro-effect locus detection and functional gene cloning, although genetic population construction and fine mapping procedures are still time-consuming (Holland 2007). As an important supplement to QTLs, association analysis based on wheat collection can simultaneously examine multiple allelic variations at the same locus, making gene localization more accurate (Breseghello and Sorrells 2006; Rafalski 2010; Atwell *et al.* 2010; Krill *et al.* 2010; Shi *et al.* 2017). The current research aim was to accurately and efficiently detect QTLs for GFR and related traits by combining linkage mapping and association analysis.

2. Materials and methods

2.1. Plant materials

The recombinant inbred line (RIL) population ($F_{8:9}$) employed in this study includes 173 lines derived from a cross between common winter wheat Shannong 01-35 and Gaocheng 9411. Shannong 01-35 is characterized by large kernels with a higher TKW (55–60 g) than Gaocheng 9411 (30–34 g) (Li *et al.* 2015). The association mapping panel used in this study was composed of 205 genetically diverse varieties or lines, 132 of which have been employed as popular varieties or backbone parents in the Chinese winter wheat area since the 1980s, while the other 73 are wheat lines from

Shandong, China (Chen *et al.* 2017; Liu *et al.* 2018).

The RIL and association mapping populations were grown in Tai'an (116°36′E, 36°57′N) in 2014–2015, 2015–2016, and 2016–2017 (E1, E2, and E3, respectively), following a randomized complete block design with two replications in each environment. Every plot consisted of four rows, and each row was 2 m long and spaced 21 cm apart. The trials were managed according to local cultivation practices.

2.2. Measurement of grain-filling traits

The specific flowering time of each variety or line was recorded. For each plot, 50 ears that bloomed on the same day were marked and five ears each were sampled at 9, 18, 27, and 36 days after flowering (DAF) (GFR_1, GFR_2, GFR_3, and GFR_4, respectively). These spikes were selected and processed by 105°C heat treatment for 10 min and drying at 60°C until a constant weight was reached. The dried samples were then measured for grain characteristics, including kernel size and grain dry weight. The GFR calculation followed the equations of Wang *et al.* (2009). A series of grain-filling parameters were derived, including the average filling rate (GFR_{mean}) and the highest filling rate (GFR_{max}).

GFD is the number of days from 75% flowering of each panicle to maturity. Two hundred grains were randomly collected from each line, and sampling was repeated three times to determine TKW. A seed processing system from Seed Processing Holland SC-G (http://www.wseen.com, Zhejiang, China) was used to process scanned spikelet images to obtain the kernel length (KL) and the kernel width (KW). To assess thickness, 20 full kernels were measured with a Vernier caliper, and the mean was taken. The measurement was repeated three times.

2.3. Genetic map and consensus map

The genetic linkage map of the RIL population and the consensus map used in the current study have been reported previously. The RIL population linkage map includes 6 244 markers (6 001 SNPs, 216 DArTs, and 27 SSRs) across 21 chromosomes covering 4 875.29 cM, with an average distance of 0.77 cM. The consensus map consists of 24 355 SNPs covering 21 chromosomes, with a total coverage of 3 674.16 cM and an average marker distance of 0.15 cM.

2.4. Statistical analysis and QTL mapping

Data management and statistical analysis were performed using SPSS 20.0 (SPSS, Chicago, IL). Analysis of variance (ANOVA) was conducted to estimate the broad-sense heritability (H^2) for each trait.

QTL analyses were implemented with QTL Network 2.0 (Yang and Zhu 2005; Yang *et al.* 2007) using the Mixed Linear Model (MLM) approach (Wang *et al.* 1999). The meaningful thresholds for QTL detection were calculated with 1 000 permutations and a genome-wide error rate of 0.05. An LOD score of 3.0 was used to verify the presence of QTLs. The data collected from the average of three environments (AE) were also used for QTL analyses. For example, *QGFR4B.3–8* indicates the 8th interval of GFR detected on chromosome 4B in this paper.

Marker-trait associations (MTAs) were identified using a MLM in Tassel 3.0, which simultaneously accounted for population structure and kinship. The population structure (summarized in the Q matrix) was inferred by Structure 2.2, and the kinship matrix (summarized in the K matrix) was calculated using the Tassel 3.0 Software. The *P*-value was used to determine whether a QTL was associated with a marker. The R^2 value was used to evaluate the magnitude of MTA effects. SNPs showing $P \leq 4.11 \times 10^{-4}$ were assumed to be significantly associated with individual traits.

3. Results

3.1. Phenotypic data

The data for grain filling-related traits assessed in the RIL and association mapping populations across different environments are shown in Tables 1, 2, and Fig. 1, respectively. The results revealed that most phenotypic values of the parent Shannon 01-35 were significantly higher than those of Gaocheng 9411 (Table 1). The differences in GFR_{max}, GFR_{mean} and TKW between the RIL population parents were 2.12 mg (grain^{-1} mg^{-1} d^{-1}), 0.76 mg (grain^{-1} mg^{-1} d^{-1}), and 30.56 g, respectively. Transgressive segregation of the grain-related traits occurred in all environments, indicating that the relevant superior alleles were randomly distributed on chromosomes.

During wheat collection, traits including KL, KW, KT, GFR, GFD, and TKW exhibited wide variation across the different environments (Table 2). Except for KL, KW, KT, and GFD, the coefficients of variation (CVs) of all other traits exceeded 12%, and the GFR in the fourth period reached 90.46%, resulting in the largest CV. The results indicated that the GFR in the fourth period presented great improvement potential and was an ideal breeding target.

The phenotypic correlations between grain-filling traits are listed in Table 3. Significant positive correlations were observed between GFR_{mean}, GFR_{max}, GFD, and TKW. The correlation between TKW and GFR_{mean} presented

Table 1 Phenotypic values of grain filling traits of the RIL population in different environments

Trait[1)]	Env.[2)]	Female Shannong 01-35	Male Gaocheng 9411	RIL[3)]					
				Min.	Max.	SD	Mean	CV (%)	H^2 (%)
GFR_1	E1	1.20	1.16	0.56	1.69	0.19	1.02	18.48	39.82
	E2	1.55	1.16	0.18	2.22	0.27	1.00	26.80	
	E3	0.68	0.64	0.37	1.01	0.11	0.64	16.37	
	AE	0.90	0.99	0.43	1.40	0.15	0.89	17.11	
GFR_2	E1	2.89	1.22	0	3.35	0.46	1.79	25.57	46.01
	E2	2.81	1.69	0.60	3.45	0.43	1.97	21.98	
	E3	2.94	1.78	–0.77	3.06	0.51	1.84	27.64	
	AE	2.94	1.56	–0.77	3.35	0.37	1.86	20.14	
GFR_3	E1	1.86	0.91	–0.90	2.79	0.67	1.42	47.47	40.62
	E2	2.72	1.11	–0.04	3.29	0.59	1.87	31.53	
	E3	2.15	1.41	–2.81	4.57	0.91	1.55	58.96	
	AE	2.12	1.14	–0.84	4.57	0.58	1.61	35.94	
GFR_4	E1	0.44	–0.48	–1.88	3.50	0.78	0.23	36.52	51.35
	E2	0.40	0.04	–2.16	2.53	0.69	0.42	63.80	
	E3	1.62	1.02	–4.38	5.33	1.19	0.67	76.53	
	AE	1.10	0.19	–1.90	2.96	0.63	0.46	36.74	
GFR_{mean}	E1	1.30	0.41	0.20	1.55	0.24	0.87	27.28	59.27
	E2	1.55	0.69	0.36	1.78	0.23	1.10	20.82	
	E3	1.71	1.12	0.70	1.71	0.18	1.11	15.88	
	AE	1.50	0.74	0.63	1.60	0.19	1.04	18.04	
GFR_{max}	E1	6.39	2.82	1.52	7.39	0.94	4.51	20.85	50.76
	E2	3.44	1.83	1.12	8.55	0.71	2.44	29.20	
	E3	3.11	1.90	0.99	6.57	0.75	2.36	31.83	
	AE	4.30	2.18	1.92	5.10	0.56	3.12	18.07	
GFD	E1	–	–	–	–	–	–	–	61.35
	E2	37.00	37.00	34.00	43.00	1.85	37.07	5.00	
	E3	39.00	39.00	36.00	42.00	1.25	38.82	3.21	
	AE	38.50	38.00	35.00	42.50	1.42	37.96	3.74	
KL	E1	8.25	6.37	6.37	8.30	0.35	7.16	4.96	74.67
	E2	7.89	6.52	6.35	7.89	0.32	7.00	4.57	
	E3	7.89	6.67	5.94	7.89	0.36	6.92	5.16	
	AE	8.03	6.52	5.79	8.03	0.34	7.00	4.84	
KW	E1	4.63	3.29	3.29	5.05	0.34	4.07	8.23	69.55
	E2	4.21	3.45	3.08	4.75	0.27	3.79	7.24	
	E3	3.92	3.72	2.94	4.78	0.28	3.80	7.47	
	AE	4.15	3.49	3.25	4.61	0.26	3.88	6.67	
KT	E1	3.03	2.24	2.17	3.42	0.24	2.72	8.72	60.74
	E2	2.97	2.84	2.49	3.36	0.18	2.89	6.08	
	E3	3.02	2.77	2.33	3.18	0.18	2.80	6.32	
	AE	2.99	2.61	2.51	3.21	0.14	2.80	4.94	
TKW	E1	57.48	25.36	13.64	66.50	8.46	40.59	20.84	65.32
	E2	57.48	25.36	13.64	66.50	8.42	40.62	20.72	
	E3	66.52	43.60	27.40	66.52	6.58	43.06	15.28	
	AE	62.00	31.44	26.73	62.00	6.82	41.64	16.39	

[1)] GFR_1, GFR_2, GFR_3, and GFR_4, grain-filling rates at 9, 18, 27 and 36 d after flowering, respectively; GFR_{mean}, the average grain-filling rate; GFR_{max}, the highest grain-filling rate; GFD, the grain-filling duration; KL, kernel length; KW, kernel width; KT, kernel thickness; TKW, thousand kernel weight.
[2)] Env., environments. E1, E2, and E3, Tai'an 2014–2015, 2015–2016, and 2016–2017, respectively; AE, the average data of three environments.
[3)] H^2, the broad-sense heritability.
–, missing data.

the highest correlation coefficient (0.97, P<0.01). KL, KW, and KT were also positively correlated with TKW, indicating that GFR was closely related to grain size.

3.2. Linkage analysis of QTL mapping

Fifty-one additive QTLs were detected in three environments

Table 2 Phenotypic values of wheat collection grain-filling traits in different environments

Trait[1)]	Env.[2)]	Min.	Max.	SD	Mean	CV (%)	H^2 (%)
GFR_1	E1	0.50	1.87	0.23	0.98	23.06	51.20
	E2	0.52	2.08	0.26	1.01	25.90	
	E3	0.28	1.98	0.18	0.64	28.31	
	AE	0.55	1.64	0.17	0.88	19.40	
GFR_2	E1	0.65	3.98	0.52	1.80	29.09	40.79
	E2	0.06	5.01	0.97	1.79	54.56	
	E3	0.05	2.85	0.42	1.52	27.82	
	AE	0.62	2.97	0.35	1.72	20.13	
GFR_3	E1	0.75	3.68	0.41	1.95	21.22	49.39
	E2	0.10	4.58	0.61	1.75	34.63	
	E3	0.18	3.82	0.54	1.85	29.41	
	AE	0.15	2.88	0.50	1.76	28.38	
GFR_4	E1	0.02	5.82	1.47	1.12	30.70	43.05
	E2	0.01	2.60	0.54	0.60	90.46	
	E3	0.10	4.96	0.85	0.89	95.30	
	AE	0.07	2.61	0.63	0.78	80.66	
GFR_{mean}	E1	0.09	1.82	0.22	1.10	20.41	64.70
	E2	0.09	1.69	0.25	1.26	20.10	
	E3	0.61	2.27	0.17	0.99	17.56	
	AE	0.37	1.61	0.18	1.12	16.04	
GFR_{max}	E1	1.20	3.24	0.43	2.12	20.31	59.52
	E2	1.27	3.62	0.46	2.38	19.50	
	E3	0.92	4.46	0.47	2.18	21.31	
	AE	1.47	4.54	0.50	2.31	21.52	
GFD	E1	30.00	42.00	2.32	35.17	6.58	53.79
	E2	30.00	42.00	2.32	35.17	6.58	
	E3	41.00	47.00	1.42	43.49	3.26	
	AE	35.50	44.50	1.66	39.33	4.22	
KL	E1	5.98	7.68	0.36	6.70	5.31	75.22
	E2	5.96	8.04	0.36	6.78	5.32	
	E3	5.79	8.05	0.38	6.61	5.80	
	AE	6.13	7.77	0.31	6.70	4.64	
KW	E1	3.13	4.33	0.24	3.75	6.36	62.16
	E2	3.09	4.54	0.27	3.81	7.04	
	E3	3.24	4.35	0.22	3.72	5.85	
	AE	3.29	4.27	0.19	3.76	5.07	
KT	E1	2.29	3.15	0.19	2.72	6.87	51.23
	E2	2.34	3.41	0.16	2.85	5.60	
	E3	2.43	3.24	0.15	2.83	5.38	
	AE	2.49	3.06	0.11	2.80	3.82	
TKW	E1	19.56	59.94	6.56	39.10	16.79	57.21
	E2	18.52	58.16	6.44	44.60	14.43	
	E3	27.70	59.90	5.91	42.77	13.82	
	AE	26.63	60.59	5.30	42.37	12.51	

[1)] GFR_1, GFR_2, GFR_3, and GFR_4, grain-filling rates at 9, 18, 27 and 36 days after flowering, respectively; GFR_{mean}, the average grain-filling rate; GFR_{max}, the highest grain-filling rate; GFD, the grain-filling duration; KL, kernel length; KW, kernel width; KT, kernel thickness; TKW, thousand kernel weight.

[2)] Env., environment. E1, E2, and E3, Tai'an 2014–2015, 2015–2016, and 2016–2017, respectively; AE, the average data of three environments.

[3)] H^2, the broad-sense heritability.

for GFR- and grain size-related traits, with PVEs of 2.15–34.75%. Among these QTLs, 15 major, stable QTLs accounted for more than 10.0% of the PVE (Table 4).

Two QTLs, *QGFR$_1$1B.7–6* and *QGFR$_1$4B.4–17*, related to GFR in the first period were detected; these were located on chromosomes 1B and 4B and displayed a PVE of 7.16 and 17.26%, respectively. Four QTLs for GFR_2 were detected and distributed on chromosomes 4B, 5B, and 6D, with PVE of 4.94–23.26%. Among these QTLs, *QGFR$_2$4B.4–13* appeared to be the major QTL for GFR_2, with a PVE of 23.26%. In the third and fourth periods, 10 QTLs were detected, including *QGFR$_3$4B.4–13* with a high PVE of 30.22%.

Four QTLs for GFR_{mean} were identified on chromosomes 4B, 5A, 5B, and 6D, with PVE ranging from 3.9 to 6.12%. Four QTLs were also detected for GFR_{max}. Among these QTLs, *QGFR$_{max}$4B.4–17* and *QGFR$_{mean}$4B.4–13* represented the two main QTLs and were both located on chromosome 4B, with PVEs of 18.65 and 34.75%, respectively. In addition, four QTLs for GFD were detected, which were distributed on chromosomes 1B, 3B, and 4B, with PVE ranging from 6.70 to 10.67%. *QGFD1B.8–70* on chromosome 1B was detected in two environments.

For grain size, 14 additive QTLs were detected, including five QTLs for the parameter KL, four for KW, and four for KT. Among these QTLs, *QKL4B.4–17*, *QKW4B.3–9*, and *QKT4B.4–17* were located on chromosome 4B, explaining 21.76, 20.77, and 17.69% of the observed variation, respectively, and seemed to be the major loci controlling grain size. In addition, nine QTLs for TKWs were detected on chromosomes 1B, 3B, 4B, 5A, 5B, and 7B, with PVE ranging from 4.74 to 33.69%. Notably, locus *4B.4–17* was detected in multiple environments with high PVE and appeared to be a major, stable QTL controlling several kernel-related traits.

3.3. Genome-wide association study of grain-filling traits

This study used 24 355 SNPs mapped to the 21 wheat chromosomes for MTA analysis. Across the three environments, 198 significant MTAs were detected for grain-filling traits. These markers were distributed across most wheat chromosomes except for 3D and 4D, with PVE ranging from 5.45–22.74% (Fig. 2; Appendix A). Among these markers, 56 showed a PVE greater than 10%.

Ten MTAs for GFR_1 were detected on eight chromosomes and showed PVE ranging from 6.96 to 11.58%. Eight highly significantly (P<0.0001) associated loci were distributed on chromosomes 1B, 3A, 3B, 4A, 5A, 5B, and 6A, with individual PVE ranging from 8.28 to 11.27%. For GFR_2, seven significant loci were detected on chromosome 5B, including *IWA8097* with a PVE of 8.27%. For GFR_3, 15 MTAs were detected and

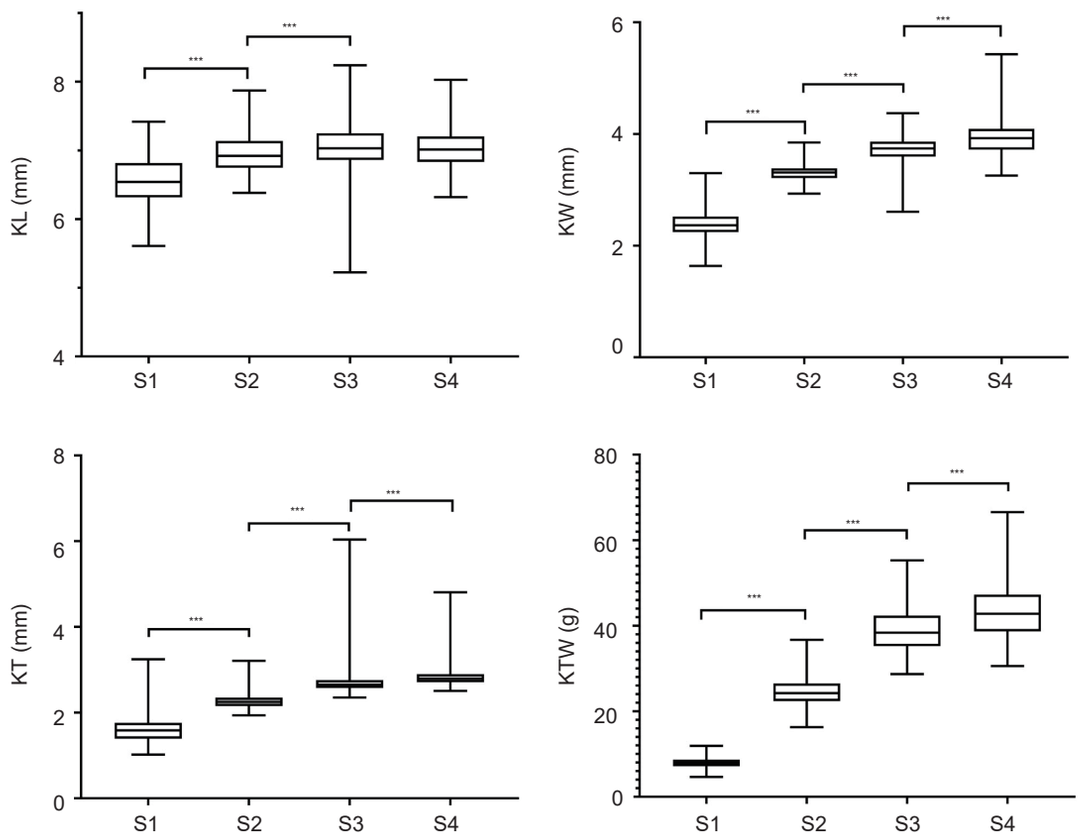

Fig. 1 Phenotypic values of grain-filling traits of the RIL population. S1–S4, 9, 18, 27 and, 36 days after flowering, respectively; KL, grain length; KW, grain width; KT, grain thickness; TKW, thousand kernel weight. ***, $P \leq 0.001$.

Table 3 Correlation analysis of grain filling traits in the RIL population[1)]

	GFR_1	GFR_2	GFR_3	GFR_4	GFR_{mean}	GFR_{max}	GFD	KL	KW	KT
GFR_1	1									
GFR_2	0.179*	1								
GFR_3	0.060	0.046	1							
GFR_4	–0.096	–0.078	–0.239**	1						
GFR_{mean}	0.067	0.347**	0.512**	0.405**	1					
GFR_{max}	0.203**	0.479**	0.419**	0.079	0.602**	1				
GFD	0.122	0.030	0.034	0.046	–0.106	0.118	1			
TKW	0.112	0.384**	0.518**	0.413**	0.970**	0.635**	0.061	0.528**	0.495**	0.555**

[1)] GFR_1, GFR_2, GFR_3, and GFR_4, grain-filling rates at 9, 18, 27 and 36 days after flowering, respectively. GFR_{mean}, the average grain-filling rate; GFR_{max}, the highest grain-filling rate; GFD, the grain-filling duration; KL, kernel length; KW, kernel width; KT, kernel thickness; TKW, thousand kernel weight.
*, $P<0.05$; **, $P<0.01$.

were mainly distributed on 1B, 2B, 4B, 5A, and 5D, with individual PVE ranging from 6.44 to 12.56%. Among these MTAs, *IWB9292* on chromosome 1B was also associated with GW. Seventeen MTAs for GFR_4 were detected on 1A, 1B, 1D, 2B, 3A, 5A, 7A, 7B, and 7D, with PVE ranging from 6.88 to 17.34%. Four loci (*IWB23316* on 1B, *IWB58600* and *IWB58601* on 7B, and *IWB49080* on 7D) were also associated with TKW. The association of the same loci with TKW and GFR indicated correlations between the GFR stage and GW.

For the GFR_{mean}, 20 MTAs were detected on chromosomes 1A, 1D, 3A, 3B, 4A, 4B, and 6B, with PVE ranging from 9.97 to 22.74%. Among these MTAs, *IWB24812* on chromosome 4B and *IWB6766* on chromosome 1D appeared to be stable MTAs and were detected in two environments. In addition, *IWB67689*, *IWB72634*, *IWB46894*, *IWB66697*, and *IWB66699* on chromosome 6B were also associated with GFD, indicating a significant correlation between GFD and GFR_{mean}. Twenty MTAs for GFR_{max} were also detected on

Table 4 Additive QTLs detected for grain filling-related traits in the RIL population[1)]

Trait[2)]	Env.[3)]	QTL	Interval	Pos (cM)	Range	*A*	*P*-value	PVE (%)
GFR_1	E1	*QGFR$_1$1B.7-6*	*IWB69144–IWB13172*	4.5	0.0–10.5	–0.05	3.28	7.16
	E2	*QGFR$_1$4B.4-17*	*IWB19555–IWB56078*	36.3	31.3–36.3	5.43	8.80	17.26
GFR_2	E1	*QGFR$_2$5B.5-488*	*IWB56335–IWA6526*	176.2	167.3–183.8	0.12	3.60	9.11
	E2	*QGFR$_2$4B.4-17*	*IWB19555–IWB56078*	36.3	21.0–36.3	0.15	7.50	19.15
	E3	*QGFR$_2$4B.4-13*	*IWB72955–IWB35996*	26.0	20.3–36.3	0.13	8.00	23.26
GFR_3	E1	*QGFR$_3$2D.1-39*	*WPT-4144–WPT-666987*	5.1	2.2–8.9	–0.16	3.94	6.83
	E1	*QGFR$_3$3A.1-104*	*IWB30389–IWB24276*	97.1	86.9–97.1	–0.17	4.10	7.33
	E1	*QGFR$_3$4B.4-13*	*IWB72955–IWB35996*	30.0	20.3–36.3	0.26	7.00	16.78
	E1	*QGFR$_3$4B.4-14*	*IWB35996–IWA500*	31.3	24.0–36.3	0.82	4.16	8.28
	AE	*QGFR$_3$4B.4-13*	*IWB72955–IWB35996*	28.0	23.0–34.3	0.29	7.00	30.22
GFR_4	E1	*QGFR$_4$2A.4-12*	*IWB45464–IWB35954*	15.5	11.3–21.6	–0.12	3.66	7.86
GFR_{mean}	E1	*QGFR$_{mean}$6D.2-3*	*IWA167–IWB54585*	11.0	7.0–17.0	0.10	3.16	6.12
GFR_{max}	E1	*QGFR$_{max}$2B.3-11*	*IWB32627–IWB7072*	24.7	0.0–25.5	0.97	1.18	2.15
	AE	*QGFR$_{max}$4B.4-13*	*IWB72955–IWB35996*	28.0	23.0–36.3	0.11	7.20	34.75
	AE	*QGFR$_{max}$4B.4-17*	*IWB19555–IWB56078*	36.3	31.3–36.3	0.24	7.00	18.65
GFD	E1	*QGFD1B.8-70*	*IWA6647–IWA2077*	85.0	77.6–86.8	–0.48	3.50	6.7
	E1	*QGFD3B.3-9*	*IWB68098–IWB7055*	12.0	0.0–17.0	0.50	3.66	7.16
	E3	*QGFD4B.8-3*	*IWB73485–IWB6896*	6.0	0.0–16.2	0.06	4.07	8.48
	AE	*QGFD1B.8-70*	*IWA6647–IWA2077*	85.0	79.6–86.8	–0.46	5.10	10.67
KL	E1	*QKL4B.4-17*	*IWB19555–IWB56078*	31.3	27.0–34.3	0.15	8.00	21.67
	E1	*QKL5A.5-3*	*IWA138–IWB11226*	3/2.7	0.0–13.8	1.15	4.40	7.37
	E2	*QKL3B.5-139*	*IWA2399–IWB2540*8	91.1	88.0–91.1	0.09	4.10	8.65
	E2	*QKL7A.4-71*	*IWB6754–IWB56584*	58.6	55.0–68.3	–0.09	4.30	9.09
	E3	*QKL5B.5-454*	*IWB67703–IWB33241*	107.0	102.6–109.7	0.11	4.80	9.62
KW	E1	*QKW3B.4-76*	*IWB42559–IWB65401*	84.0	80.9–87.9	0.09	6.00	8.39
	E1	*QKW4B.3-9*	*IWB59993–IWB73001*	27.4	22.4–28.4	0.14	6.70	20.77
	E1	*QKW4B.5-115*	*IWB42664–IWB52747.1*	71.7	66.8–79.7	0.07	4.20	5.72
	E3	*QKW4B.4-17*	*IWB19555–IWB56078*	36.3/34.3	33.3–36.3	0.13	6.00	13.38
KT	E1	*QKT4B.4-3*	*IWB12856–IWB35611*	3.3	0.0–17.6	0.13	2.80	22.59
	E3	*QKT1A.1-18*	*WPT-4029–WPT-8455*	46.1	40.0–46.1	0.04	3.90	5.63
	E3	*QKT4B.4-17*	*IWB19555–IWB56078*	33.3	27.0–36.3	0.07	6.50	17.69
	E3	*QKT7A.1-20*	*IWA3850–IWB7997*	23.1	21.6–24.9	–0.04	4.50	6.77
TKW	E1	*QTKW1B.8-70*	*IWB19555–IWB56078*	33.3	25.0–36.3	3.06	5.10	11.69
	E1	*QTKW4B.4-17*	*IWB19555–IWB56078*	35.3	25.0–36.3	3.98	7.00	23.12
	E2	*QTKW1B.8-70*	*IWA6647–IWA2077*	85.0	77.6–86.8	–0.48	3.50	6.70
	E2	*QTKW3B.3-9*	*IWB68098–IWB7055*	12.0	0.0–17.0	0.50	3.66	7.16
	E3	*QTKW1B.8-75*	*IWB64714.1–IWB73820*	85.8	77.6–86.8	–0.37	5.05	8.91
	E3	*QTKW5A.10-6*	*IWA5929–WPT-3334*	6.9	0.0–16.5	0.41	5.70	10.57
	E3	*QTKW5B.5-362*	*IWB20240–IWB6590.2*	30.4	26.9–33.5	–0.37	4.96	8.85
	AE	*QTKW4B.4-17*	*IWB19555–IWB56078*	34.3	31.3–36.3	3.86	8.00	33.69

[1)] Env., environment; Pos, position; *A*, additive effects, a positive value indicates an allele from Shannong 01-35, and a negative value indicates an allele from Gaocheng 9411; PVE, phenotypic variation explained.
[2)] GFR_1, GFR_2, GFR_3, and GFR_4, grain-filling rates at 9, 18, 27 and 36 days after flowering, respectively; GFR_{mean}, the average grain-filling rate; GFR_{max}, the highest grain-filling rate; GFD, the grain-filling duration; KL, kernel length; KW, kernel width; KT, kernel thickness; TKW, thousand kernel weight.
[3)] E1, E2, and E3, Tai'an 2014–2015, 2015–2016, and 2016–2017, respectively; AE, the average data of three environments.

chromosomes 1B, 2B, 3B, 4A, 5A, 6A, 6B, 6D, 7B, and 7D, with PVE ranging from 5.45 to 11.69%. Among these MTAs, *IWB7662* (*P*<0.0001) showed the highest PVE of 11.69%.

Fifteen MTAs were associated with KL and located on chromosomes 1A, 1B, 2D, 4B, 5B, and 7A, with individual PVE of 6.7–10.94%. Among these MTAs, *IWA4726* on chromosome 5B showed high significance in two environments. Sixteen MTAs for KW were mainly identified on chromosomes 1B, 4B, 5B, and 7A, with PVE ranging from 5.76 to 10.94%. Twenty-one MTAs for KT were also detected on chromosomes 1A, 1B, 2B,

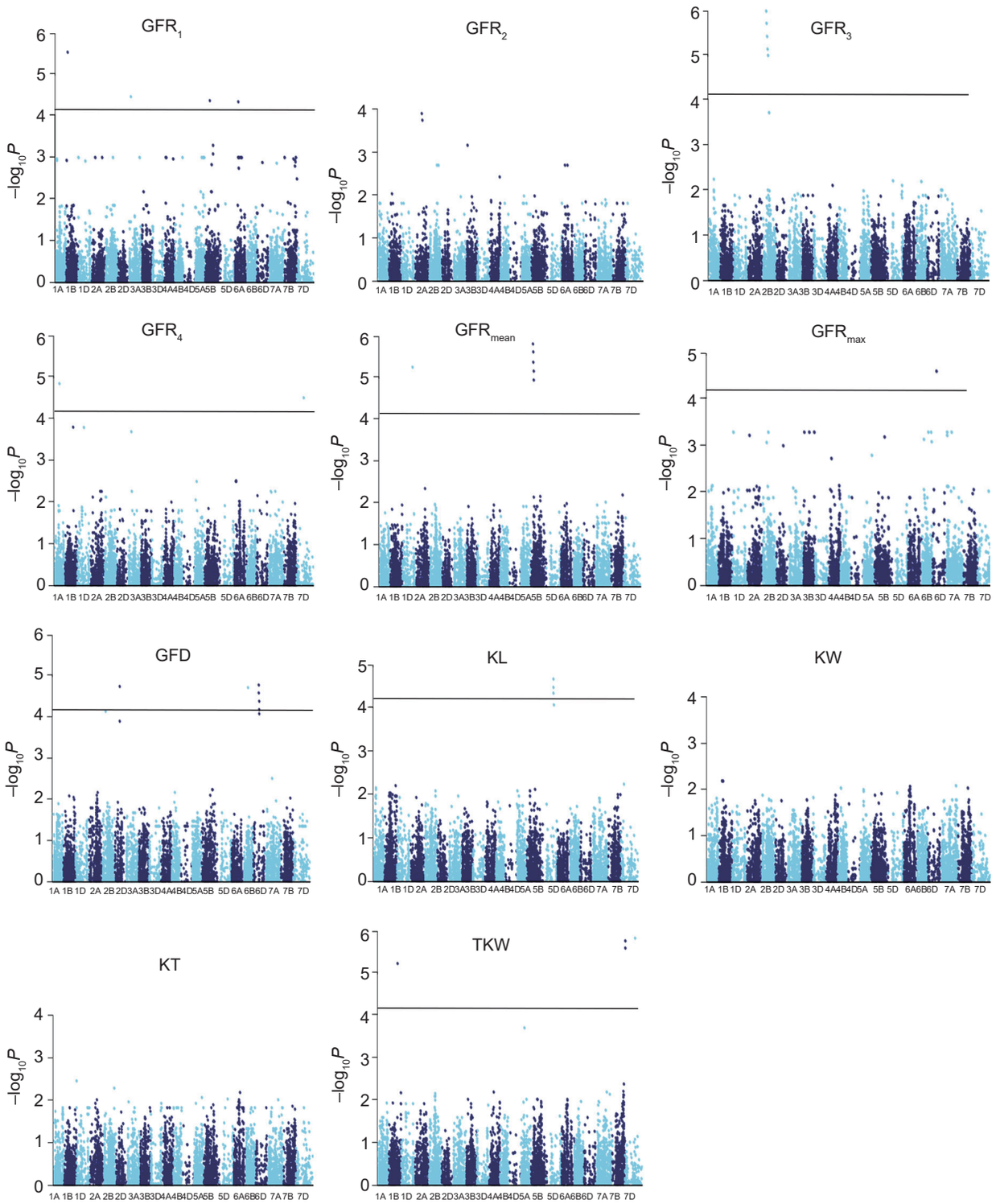

Fig. 2 Manhattan plots of grain filling-related traits. GFR_1, GFR_2, GFR_3, and GFR_4, grain-filling rates at 9, 18, 27 and 36 days after flowering, respectively; GFR_{mean}, the average grain-filling rate; GFR_{max}, the highest grain-filling rate; GFD, grain-filling duration; KL, kernel length; KW, kernel width; KT, kernel thickness; TKW, thousand kernel weight.

2D, 3A, 4B, 5B, 6D, 7A, and 7B, with PVE of 6.8–11.9%. Among these MTAs, *IWB72009* on chromosome 4B was associated with GRF_4, KL, KW, and KT, indicating that it is a pleiotropic locus that controls grain size. Furthermore, 25 MTAs for TKW were mainly detected on chromosomes 1B, 2B, 4A, 4B, 5A, 5B, 6D, 7A, 7B, and 7D. Among

these MTAs, *IWB11820* located on chromosome 1B exhibited the highest PVE of 12.98%, while two MTAs (*IWA7795* on 5B and *IWA5081* on 2B) showed stable correlations, as they were detected under different environmental conditions.

4. Discussion

4.1. Advantage of combined linkage and association analysis

Sequencing and genotyping technologies have developed rapidly over the past decade. With the development of SNP arrays, this technology has been widely applied in polyploid crops such as wheat (Edwards *et al.* 2013). Additionally, powerful statistical analysis tools have promoted the rapid progress of QTL mapping of important agronomic traits, such as yield, panicle architecture, and plant architecture.

QTL mapping based on genetic linkage maps has been successfully applied in the mapping of important quantitative traits in wheat (Ma *et al.* 2005, 2007; Wu *et al.* 2016). Nevertheless, this method requires the construction of a genetic population according to the target traits, and the polymorphism of molecular markers is affected by the genetic background of the population parents (Li *et al.* 2018; Duan *et al.* 2020; Mangini *et al.* 2021). GWAS, based on linkage disequilibrium, is a powerful tool for detecting all genetic effects at loci involved in the expression of target traits (Shu and Rasmussen 2014; Rajiv *et al.* 2018) and offers the possibility of identifying all recombination events. However, this method is susceptible to the influence of group structure and the risk of producing false associations between markers and traits. Therefore, the combined use of the two methods can improve the accuracy of the detection of favorable variation and provide a better understanding of the relationships between targeted traits. For example, *IWB35850*, identified through GWAS, was located in approximately the same region as $QGFR_{max}2B.3–11$ by linkage analysis, and this region contained two high-confidence candidate genes. *IWA7795* and *QTKW5B.5–362* were located in adjacent regions of the same chromosome, and these associations were detected in multiple environments. Six markers (*IWB13069*, *IWB10098*, *IWA5589*, *IWA6654*, *IWB42573*, and *IWB59901*) associated with GFR_{max} were located on the marker interval (*Xgpw4142–Xbarc113*) by linkage analysis.

4.2. Important gene loci for GFR

In the current study, through QTL mapping, four QTLs for GFR_{mean} were identified, which were located on chromosomes 4B, 5A, 5B, and 6D. Through GWAS, significant association sites for GFR_{mean} were identified on chromosomes 1A, 1D, 3A, 3B, 4A, 4B, and 6B, with PVE ranging from 9.97 to 22.74%. Chromosome 4B was found to harbor two QTLs for GFR_{mean} in both analyses.

Of the QTLs controlling GFR_{max} in the linkage analysis, $QGFR_{max}4B.4–17$ and $QGFR_{mean}4B.4–13$, both located on chromosome 4B, had high PVE and were the main and stable QTLs for the filling rate. In the association analysis, the highly significantly associated sites controlling GFR_{max} were mainly distributed on chromosomes 1B, 2B, 5A, 5D, 6B, and 6D, with PVE of 10.58–11.69%. Notably, *IWB35850* on 2B, detected in the GWAS, is located in approximately the same region as $QGFR_{max}2B.3–11$, identified in the linkage analysis, with a physical distance of only 6.3 Mb; this interval contains two high-confidence candidate genes, *TraesCS2B01G122100* and *TraesCS2B01G122900*. *TraesCS2B01G122100* encodes an expansion protein that affects cell wall loosening, plant growth and development, and reactions to plant diseases and other stresses (Fleming *et al.* 1997; Zhang J F *et al.* 2018). Furthermore, a gene prediction website (https://wheat.pw.usda.gov/WheatExp/) revealed that *TraesCS2B01G122900* expression can reach 15.8 and 16.5 FPKM (fragments per lilobase million) in the grain filling and flag leaf development stages of wheat growth, respectively (Appendix B). Since most of the dry matter in wheat grains comes from photosynthesis in flag leaves and ears (Evans and Rawson 1970), this gene is logically a potential candidate gene.

For KL, the stable QTL *QKL4B.4–17* with high PVE (21.67%) was detected in multiple environments. In association analysis, three extremely significant association sites (*IWA4726*, *IWB142*, and *IWB12805*) were distributed on the same chromosome, 5B. Additionally, *IWA4726* was stably detected in both environments. *QKW4B.4–17*, *QKW4B.5–115*, and *QKW4B.3–9* were detected in a variety of environments and appeared to be stable QTLs with relatively stronger effects on KW. Four highly significantly (P<0.0001) related loci (*IWB28146*, *IWB64503*, *IWB30048*, and *IWB47520*) were detected on 5B. Four highly significant loci (*IWB10628*, *IWB4395*, *IWB63985*, and *IWB65764*) associated with KT (P<0.0001) were detected on 7B.

QTKW4B.4–17 and *QTKW4B.4–13* were identified as important QTL sites controlling TKW. According to combined linkage and association analysis, the key genes controlling grain size and GW were mainly located on chromosomes 4B and 5B. In contrast, we found that *IWA7795* (9.27%) and *QTKW5B.5–362* were located in adjacent regions of the same chromosome, and these associations were repeated in multiple environments.

Hai *et al.* (2008) used a double haploid (DH) population generated from CA9613/H1488 and 168 SSR markers to analyze the number of spikes, kernel weight, and TKW in four ecological environments. Thirty QTLs were detected, located on chromosomes 1A, 1B, 2B, 2D, and 7D. Ma *et al.* (2007) located QTLs for spike length and spikelet density on 2DS. Kumar *et al.* (2007) detected QTLs controlling grain yield, the harvest index, panicle length, total spikelet number, and kernel number on 2DS. The lack of consistency between these findings and the current study's findings suggests that there are more genes/QTLs for TKW in addition to those reported in the current study.

4.3. Comparison of the present study with previous research

The average wheat GFR and the highest GFR are two important parameters in grain development and are also important factors affecting grain yield characteristics (Wang R X *et al.* 2008). However, few relevant QTL mapping studies have been conducted due to the cumbersome methods required for determining grain-filling traits (Kirigwi *et al.* 2007). A previous study examining a recombinant inbred population under drought conditions located a QTL affecting GFR in the *xwmc89*–*xwmc420* region of chromosome 4A (Kirigwi *et al.* 2007). However, the QTLs for GFR identified in the current study were mainly located on chromosomes 1B, 4B, and 6A. This difference may be due to the different genetic materials used. In addition, 26 QTLs for the final GW, 13 for carpel size, and 81 for grain dry matter accumulation were previously detected in a Forno×Oberkulmer mapping population over two years (Xie *et al.* 2015). Among these QTLs, the chromosomal locations of the markers (*Xpsr1327b-1A*, *Xpsr168-1DS*, *Xpsr1196b-3BXglk315-4AS*, and *Xpsr918b-5A*) for GFR_{mean} and GFR_{max} were cross-verified in different populations in our study. In addition, six markers (*IWB13069*, *IWB10098*, *IWA5589*, *IWA6654*, *IWB42573*, and *IWB59901*) associated with GFR_{max} were located on the marker interval (*Xgpw4142*–*Xbarc113*) by linkage analysis.

So far, more than 100 QTLs controlling wheat grain weight have been reported, with 51 having a PVE over 10%. The main QTLs were located on 1A (Kumari *et al.* 2019), 4DS (Jia *et al.* 2013), 5A (Brinton *et al.* 2017), 6A (Hanif *et al.* 2016), and 7AL (Su *et al.* 2016). Numerous studies have shown that there are important gene loci for grain traits on 4B (Williams and Sorrells 2014; Li *et al.* 2015). These include *QTkw.macs-4B.2* (Patil *et al.* 2013) and *QGw.nau-4B* (Huang *et al.* 2015). *QTgw.crc-4BL*, *QTgw.wa-4BL.e2* and *QTkwpk.cimmyt-4BL* were located on the long arm of 4B (Wang *et al.* 2011; Hao *et al.* 2014). Through comparison, our QTL *TaGW4B* is more than 10 Mb apart from the above QTLs, and they have different positioning intervals.

In this study, QTLs for KL, KW, KT, and TKW were identified on chromosome 4B. In a previous study, a DH population with 225 lines from a cross between Westonia and Kauz was used to identify grain phenotypes, including GW, TKW, and KN, in three environments using 9K SNPs, 195 SSR markers, and *Rht* gene markers (Ellis *et al.* 2002). Highly significant QTLs for TKW and KN were detected on chromosomes 4B and 4D in the *Rht-B1a* and *Rht-D1a* regions, respectively (Zhang J J *et al.* 2013). Later, based on a new 90K SNP WK map, a significant TKW QTL (LOD>10) was identified on the 4B long arm, 55 cM below*Rht-B1b* (*Rht1*), while separate QTLs for GW and KN were found at and close to the *Rht-B1b* (*Rht1*) gene on 4BS (Appendix C). GW and TKW QTLs were both mapped in the current study. The peak of the TKW QTL in the Westonia×Kauz population is located at 570.2 Mb on 4BL in the Chinese Spring physical map (*IWGSC_RefSeq_v1.0*). By using different genetic populations, the current study also detected this TKW QTL on 4BL between 480.6 and 612.2 Mb through both QTL mapping and GWAS. The Westonia×Kauz QTL region included 10 genes. Ahmed *et al.* (2018) predicted a candidate gene for this QTL, the sucrose transporter gene *TaSUT1_4B* and our team are currently conducting a series of experiments to study the mechanism of this gene underlying the TKW QTL. A grain-filling QTL was also located in this region in the current study, indicating that the high-TKW phenotype is conferred through an enhanced GFR. This further supports our prediction from candidate gene analysis that sucrose transporter alleles enhance sucrose transfer from vegetative organs to seeds, resulting in a higher GFR and consequently a high TKW.

In the current study, a pleiotropic QTL for GFR, TKW, KL, KW, and KT was identified on chromosome 4BS in the interval from 28.9 to 36.6 Mb in the Chinese Spring physical map (*Wheat_IWGSC_RefSeq_v1.0*). This is consistent with the GW QTL identified in the Westonia×Kauz population and the TGW QTL reported by Xu *et al.* (2019). The current study located a stable GFR QTL in this region and once again confirmed that the GW phenotype associated with this chromosome region is caused by variation in grain filling. Nine high-confidence genes, including *Rht1* (4B: 30.8 Mb), were located in this region. The two genes closest to *Rht-B1b* (*Rht1*) (*TraesCS4B02G042900* (*ZnF*) and *TraesCS4B02G043000* (*EamA*)) were recently predicted as potential candidate genes for the TGW QTL (Xu *et al.*

2019). *EamA* (*PF00892*) is located at cell membranes and acts as a metabolite transporter. This function is in accordance with the GFR data from the current study. Therefore, *EamA* is a more likely candidate gene for the QTL on chromosome 4BS. T_0 generation-positive transgenic plants were obtained through genetic transformation. The qRT-PCR results showed higher gene expression levels in over-expression plants, which was in accordance with the higher grain weight. We speculated that *EamA* is related to kernel development. Because few seeds in theT_0 generation were harvested, the grain filling rate had to be further verified in the T_1 and T_2 generations.

5. Conclusion

The study used linkage and association analyses to identify a few stable and important QTL clusters associated with GFRs. These QTLs may be of great value for marker-assisted selection in wheat breeding. In addition, the application of two bioinformatics methods provided new insights into the genetic mechanisms and regulatory networks of complex traits in wheat.

Acknowledgements

This work was supported by the National Natural Science Foundation of China (31971936) and the Science &Technology Projects of Shandong Province, China (2019YQ028, 2020CXGC010805, 2019B08, 2019YQ014 and ZR2020MC093). SNP analysis and the construction of genetic maps were kindly conducted by Dr. Luo Mingcheng from the University of California, Davis, and by Dr. Wang Jirui from Sichuan Agricultural University.

Declaration of competing interest

The authors declare that they have no conflict of interest.

Appendices associated with this paper are available on http://www.ChinaAgriSci.com/V2/En/appendix.htm

References

Ahmed A S, Zhang J, Ma W, Dell B. 2018. Contributions of *TaSUTs* to grain weight in wheat under drought. *Plant Molecular Biology*, **98**, 4–5.

Alonso M P, Abbate P E, Mirabella N E, Merlos F A, Panelo J S, Pontaroli A C. 2018. Analysis of sink/source relations in bread wheat recombinant inbred lines and commercial cultivars under a high yield potential environment. *European Journal of Agronomy*, **93**, 82–87.

Atwell S, Huang Y S, Vilhjalmsson B J, Willems G, Horton M, Li Y, Meng D Z, Platt A, Tarone A M, Hu T T, Jiang R, Muliyati N W, Zhang X, Amer M A, Baxter I, Brachi B, Chory J, Dean C, Debieu M, Meaux J D, *et al.* 2010. Genome-wide association study of 107 phenotypes in *Arabidopsis thaliana* inbred lines. *Nature*, **465**, 627–631.

Baillot N, Girousse C, Allard V, Piquet-Pissaloux A, Gouis J L. 2018. Different grain-filling rates explain grain-weight differences along the wheat ear. *PLoS ONE*, **13**, e0209597.

Breseghello F, Sorrells M E. 2006. Association mapping of kernel size and milling quality in wheat (*Triticum aestivum* L.) cultivars. *Genetics*, **172**, 1165–1177.

Brinton J, Simmonds J, Minter F, Leverington-Waite M, Snape J, Uauy C. 2017. Increased pericarp cell length underlies a major quantitative trait locus for grain weight inhexaploid wheat. *New Phytologist*, **215**, 1026–1038.

Chen G F, Wu R G, Li D M, Yu H X, Deng Z, Tian J C. 2017. Genomewide association study for seeding emergence and tiller number using SNP markers in an elite winter wheat population. *Journal of Genetics*, **96**, 177–186.

Consortium T. 2014. A chromosome-based draft sequence of the hexaploid bread wheat (*Triticum aestivum* L.) genome. *Science*, **345**, 1251788.

Dfreynolds M C. 2000. Changes in grain weight as a consequence of de-graining treatments at pre- and post-anthesis in synthetic hexaploid lines of wheat (*Triticum durum*×*T. tauschii*). *Australian Journal of Plant Physiology*, **27**, 183–191.

Dobrovolskaya O, Pont C, Sibout R, Martinek P, Badaeva E, Murat F, Chosson A, Watanable N, Prat E, Gauter N, Gautier V, Poncet C, Orlov T L, Krasnikov A A, Berges H, Salina E, Laikova L, Salse J. 2015. Frizzy panicle drives supernumerary spikelets in bread wheat. *Plant Physiology*,**167**, 189–199.

Du B B, Wang Q F, Sun G L, Ren X F , Cheng Y, Wang Y X, Gao S, Li C D, Sun D F. 2019. Mapping dynamic QTL dissects the genetic architecture of grain size and grain filling rate at different grain-filling stages in barley. *Scientific Reports*, **9**, 18823.

Duan X X, Yu H X, Ma W J, Sun J Q, Zhao Y, Yang R C, Ning T Y, Li Q F, Liu Q Q, Guo T T, Yan M, Tian J C, Chen J S. 2020. A major and stable QTL controlling wheat thousand grain weight: Identification, characterization, and CAPS marker development. *Molecular Breeding*, **40**, 68.

Edwards D, Batley J, Snowdon R J. 2013. Accessing complex crop genomes with next-generation sequencing. *Theoretical and Applied Genetics*, **126**, 1–11.

Ellis H, Spielmeyer W, Gale R, Rebetzke J, Richards A. 2002. “Perfect” markers for the *Rht-B_1b* and *Rht-D_1b* dwarfing genes in wheat. *Theoretical and Applied Genetics*, **105**, 1038–1042.

Evans L T, Rawson H M. 1970. Photosynthesis and respiration by the flag leaf and components of the ear during grain development in wheat. *Australian Journal of Biological Sciences*, **23**, 245–254.

Fischer R A. 2008. The importance of grain or kernel number

in wheat: A reply to sinclair and jamieson. *Field Crops Research*, **105**, 15–21.

Fischer T. 2011. Wheat physiology: A review of recent developments. *Crop and Pasture Science*, **62**, 95–114.

Fleming A J, Mcqueen-Mason S, Mandel T, Kuhlemeiert C. 1997. Induction of leaf primordia by the cell wall protein expansin. *Science*, **276**, 1415–1418.

Gupta P K, Rustgi S, Kumar N. 2006. Genetic and molecular basis of grain size and grain number and its relevance to grain productivity in higher plants. *Genome*, **49**, 565–571.

Hai L, Guo H J, Wagner C, Xiao S H, Friedt W. 2008. Genomic regions for yield and yield parameters in Chinese winter wheat (*Triticum aestivum* L.) genotypes tested under varying environments correspond to QTL in widely different wheat materials. *Plant Science*, **175**, 226–232.

Hanif M, Gao F, Liu J, Wen W, Zhang Y, Rasheed A, Xia X, He Z, Cao S. 2016. *TaTGW6-A1*, an ortholog of rice *TGW6*, is associated with grain weight and yield in breadwheat. *Molecular Breeding*, **36**, 1.

Hao Y, Velu G, Peña R, Singh S, Singh R. 2014. Genetic loci associated with high grain zinc concentration and pleiotropic effect on kernel weight in wheat (*Triticum aestivum* L.). *Molecular Breeding*, **34**, 1893–1902.

Holland J B. 2007. Genetic architecture of complex traits in plants. *Current Opinion in Plant Biology*, **10**, 156–161.

Huang Y, Kong Z, Wu X, Cheng R, Yu D, Ma Z. 2015. Characterization of three wheat grain weight QTLs that differentially affect kernel dimensions. *Theoretical and Applied Genetics*, **128**, 2437–2445.

Jia H, Wan H, Yang S, Zhang Z, Kong Z, Xue S, Zhang L, Ma Z. 2013. Genetic dissection of yield-related traits in a recombinant inbred line population created using a key breeding parent in China's wheat breeding. *Theoretical and Applied Genetics*, **126**, 2123–2139.

Kirigwi F M, Ginkel M V, Brown-Guedira G, Gill B S, Fritz A K. 2007. Markers associated with a QTL for grain yield in wheat under drought. *Molecular Breeding*, **20**, 401–413.

Knott D R, Gebeyehou G. 1987. Relationships between the lengths of the vegetative and grain filling periods and agronomic characters in three durum wheat crosses. *Crop Science*, **27**, 857–860.

Krill A M, Kirst M, Kochian L V, Buckler E S, Hoekenga O A. 2010. Association and linkage analysis of aluminum tolerance genes in maize. *PLoS ONE*, **5**, e9958.

Kumar N, Kulwal P L, Balyan H S, Gupta P K. 2007. QTL mapping for yield and yield contributing traits in two mapping populations of bread wheat. *Molecuar Breeding*, **19**, 163–177.

Kumari S, Mir R R, Tyagi S, Balyan H S, Gupta P K. 2019. Validation of QTL for grain weight using MAS-derived pairs of NILs in bread wheat (*Triticum aestivum* L.). *Journal of Plant Biochemistry and Biotechnology*, **28**, 336–344.

Li F J, Wen W , He Z H , Liu J D, Jin H, Cao S H, Geng H W, Yan J, Zhang P Z, Wan Y X, Xia X C. 2018. Genome-wide linkage mapping of yield-related traits in three Chinese bread wheat populations using high-density SNP markers. *Theoretical and Applied Genetics*, **131**, 1903–1924.

Li M, Li X X, Zhou Z J, Wu P Z, Fang M C, Pan X P, Lin Q P, Luo W B, Wu G J, Li H Q. 2016. Reassessment of the four yield-related genes *Gn1a*, *DEP1*, *GS3*, and *IPA1* in rice using a CRISPR/Cas9 System. *Frontiers in Plant Science*, **7**, 377.

Li Q F, Zhang Y, Liu T T, Wang F F, Liu K, Chen J S, Tian J S. 2015. Genetic analysis of kernel weight and kernel size in wheat (*Triticum aestivum* L.) using unconditional and conditional QTL mapping. *Molecular Breeding*, **35**, 194.

Li W L, Gill B S. 1970. *Genomics for Cereal Improvement*. Cereal Genomics, Netheriands. pp. 585–634.

Liu K, Sun X X, Ning T Y, Duan X X, Wang Q L, Liu T T, An Y L, Gaun X, Tain J C, Chen J S. 2018. Genetic dissection of wheat panicle traits using linkage analysis and a genome-wide association study. *Theoretical and Applied Genetics*,**131**, 1073–1090.

Ma W, Appels R, Bekes F, Larroque O, Morell M K, Gale K R. 2005. Genetic characterisation of dough rheological properties in a wheat doubled haploid population: Additive genetic effects and epistatic interactions. *Theoretical and Applied Genetics*, **111**, 410–422.

Ma Z Q, Zhao D M, Zhang C Q, Zhang Z Z, Xue S L, Lin F, Kong Z X, Tian D G, Luo Q Y. 2007. Molecular genetic analysis of five spike-related traits in wheat using RIL and immortalized F_2 populations. *Molecular Genetics and Genomics*, **277**, 31–42.

Mangini G, Blanco A , Nigro D , Signorile M A , Simeone R. 2021. Candidate genes and quantitative trait loci for grain yield and seed size in durum wheat. *Plants* (Basel), **10**, 312.

Mashiringwani N A, Mashingaidze K, Kangai J, Olsen K. 1994. Genetic basis of grain filling rate in wheat (*Triticum aestivum* L. emend. Thell.). *Euphytica*, **76**, 33–44.

Patil R M, Tamhankar S A, Oak M D, Raut A L, Honrao B K, Rao V S, Misra S C. 2013. Mapping of QTL for agronomic traits and kernel characters in durum wheat (*Triticum durum* desf.). *Euphytica*, **190**, 117–129.

Rafalski J A. 2010. Association genetics in crop improvement. *Current Opinionin Plant Biology*, **13**, 174–180.

Rajiv S, Fulvia B, Hazel B, Paul H, Andreas M, Klaus P, Thomas W T B, FlavellA J. 2018. Genome-wide association of yield traits in a nested association mapping population of barley reveals new gene diversity for future breeding. *Journal of Experimental Botany*, **69**, 3811–3822.

Sanford D. 1985. Variation in kernel growth characters among soft red winter wheats. *Crop Science*, **25**, 626–630.

Shi W P, Hao C Y, Zhang Y, Cheng J Y, Zhang Z, Liu J, Yi X, Cheng X M, Sun D Z, Xu Y H, Zhang X Y, Cheng S H, Guo P Y, Guo J. 2017. A combined association mapping and linkage analysis of kernel number per spike in common wheat (*Triticum aestivum* L.). *Frontiers in Plant Science*, **8**, 1412.

Shu X L, Rasmussen S K. 2014. Quantification of amylose, amylopectin, and β-glucan in search for genes controlling the three major quality traits in barley by genome-wide association studies. *Frontiers in Plant Science*, **5**, 197.

Su Z, Jin S, Lu Y, Zhang G, Chao S, Bai G. 2016. Single

nucleotide polymorphism tightly linked to a major QTL on chromosome 7A for both kernel length and kernel weight in wheat. *Molecular Breeding*, **36**, 15.

Tollenaar M, Lee E A. 2006.Dissection of physiological processes underlying grain yield in maize by examining genetic improvement and heterosis. *Maydica*, **51**, 399–408.

Wang D L, Zhu J, Li Z K, Paterson A H. 1999. Mapping QTL with epistatic effects and QTL×Environment interactions by mixed linear model approaches. *Theoretical and Applied Genetics*, **99**, 1255–1264.

Wang E T, Wang J J, Zhu X D, Hao W, Wang L Y, Li Q, Zhang L X, He W, Lu B R, Lin H X, Ma H, Zhang G Q, He Z H. 2008. Control of rice grain-filling and yield by a gene with a potential signature of domestication. *Nature Genetics*, **40**, 1370–1374.

Wang J, Liu W, Wang H, Li L, Wu J, Yang X, Li X, Gao A. 2011. QTL mapping of yield-related traits in the wheat germplasm 3228. *Euphytica*, **177**, 277–292.

Wang R X, Hai L, Zhang X Y, You G X, Yan C S, Xiao S H. 2009. QTL mapping for grain filling rate and yield-related traits in RILs of the Chinese winter wheat population Heshangmai × Yu8679. *Theoretical and Applied Genetics*, **118**, 313–325.

Wang R X, Zhang X Y, Wu L, Wang R, Hai L, Yan C S, You G X, Xiao S H. 2008. QTL mapping for grain filling rate and thousand-grain weight in different ecological environments in wheat. *Acta Agronomica Sinica*, **34**, 1750–1756. (in Chinese)

Wang S K, Wu K, Yuan Q B, Liu X Y, Liu Z B, Lin X Y, Zeng R Z, Zhu H T, Dong G J, Qian Q, Zhang G Q, Fu X D. 2012. Control of grain size, shape and quality by *OsSPL16* in rice. *Nature Genetics*, **44**, 950–954.

Wiegand C L, Cuellar J A. 1981. Duration of grain filling and kernel weight of wheat as affected by temperature. *Crop Science*, **21**, 95–101.

Williams K, Sorrells M E. 2014. Three-dimensional seed size and shape QTL in hexaploid wheat (*Triticum aestivum* L.) populations. *Crop Science*, **54**, 98–110.

Wu Q H, Chen Y X, Fu L, Zhou S H, Chen J J, Zhang D, Quan S H, Wang Z Z, Li D, Wang G X, Zhang D Y, Yuan C G, Wang L X, You M S, Han J, Zhao X Y. 2016. QTL mapping of flag leaf traits in common wheat using an integrated high-density SSR and SNP genetic linkage map. *Euphytica*, **208**, 337–351.

Xie Q, Mayes S, Sparke D L. 2015. Carpel size, grain filling, and morphology determine individual grain weight in wheat. *Journal of Experimental Botany*, **66**, 6715–6730.

Xu D G, Wen W, Fu L P, Li F J, Li J H, Xie L, Xia X C, Ni Z F, He Z H, Cao S H. 2019. Genetic dissection of a major QTL for kernel weight spanning the *Rht-B1* locus in bread wheat. *Theoretical and Applied Genetics*, **132**, 3191–3200.

Yang J, Zhu J. 2005. Methods for predicting superior genotypes under multiple environments based on QTL effects. *Theoretical and Applied Genetics*, **110**, 1268–1274.

Yang J, Zhu J, Williams RW. 2007.Mapping the genetic architecture of complex traits in experimental populations. *Bioinformatics*, **23**, 1527–1536.

Yano M. 2001. Genetic and molecular dissection of naturally occurring variation. *Current Opinionin Plant Biology*, **4**, 130–135.

Zhang D, Wang B, Zhao J, Zhao X, Zhang L, Liu D, Dong L, Wang D, Mao L, Li A. 2015. Divergence in homoeolog expression of the grain length-associated gene *GASR7* during wheat allohexaploidization. *The Crop Journal*, **3**, 1–9.

Zhang J F, Xu Y Q, Dong J M, Peng L N, Feng X, Wang X, Li F, Miao Y, Yao S K, Zhao Q Q, Feng S S, Hu B Z, Li F L. 2018. Genome-wide identification of wheat (*Triticum aestivum* L.) expansins and expansion expression analysis in cold-tolerant and cold-sensitive wheat cultivars. *PLoS ONE*, **13**, e0195138.

Zhang J J, Dell B, Biddulph B, Drake-Brockman F, Walker E, Khan N, Wong D, Hayden M, Appels R. 2013. Wild-type alleles of *Rht-B1* and *Rht-D1* as independent determinants of thousand-grain weight and kernel number per spike in wheat. *Molecular Breeding*, **32**, 771–783.

Zhang Y, Li D, Zhang D, Zhao X, Cao X, Dong L, Liu J, Chen K, Zhang H, Gao C. 2018. Analysis of the functions of TaGW2 homoeologs in wheat grain weight and protein content traits. *Plant Journal for Cell and Molecular Biology*, **94**, 857–866.

Zhang Z H, Liu ZH, Cui Z T, Hu Y M, Wang B, Tang J H. 2013. Genetic analysis of grain filling rate using conditional QTL mapping in maize. *PLoS ONE*, **8**, e56344.

Zhu D M, Wang H, Liu D T, Gao D R, Lu G F, Wang J C, Gao Z F, Lu C B. 2019. Characteristics of grain filling and dehydration in wheat. *Scientia Agricultura Sinica*, **52**, 4251–4261. (in Chinese)

Executive Editor-in-Chief ZHANG Xue-yong
Managing Editor WANG Ning